

pubs.acs.org/JPCB Perspective

# Short Peptides as Tunable, Switchable, and Strong Gelators

Reinhard Schweitzer-Stenner\* and Nicolas J. Alvarez



Cite This: J. Phys. Chem. B 2021, 125, 6760-6775

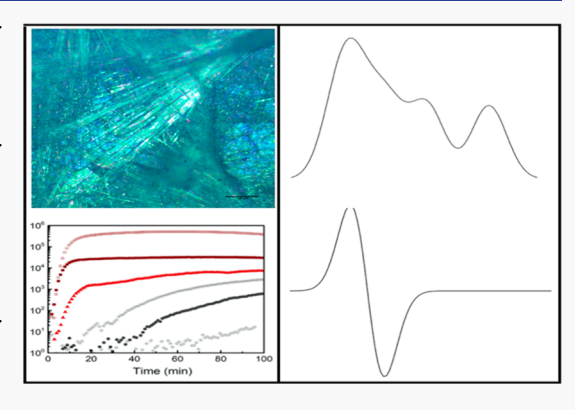


**ACCESS** I

Metrics & More

Article Recommendations

**ABSTRACT:** This Perspective outlines our current understanding of molecular gels composed of short and ultrashort peptides over the past 20 years. We discuss in detail the state of the art regarding self-assembly mechanisms, structure, thermal stability, and kinetics of fibril and/or network formation. Emphasis is put on the importance of the combined use of spectroscopy and rheology for characterizing and validating self-assembly models. While a range of peptide chemistries are reviewed, we focus our discussion on a unique new class of ultrashort peptide gelators, denoted GxG peptides (x: guest residue), which are capable of forming self-assembled fibril networks. The storage moduli of GxG gels are tunable up to 100 kPa depending on concentration, pH, and/or cosolvent. The sheet structures of the fibrils differ from canonical  $\beta$ -sheets. When appropriate, each section highlights opportunities for additional research and technologies that would further our understanding.



# ■ SHORT AND ULTRASHORT PEPTIDE GELATORS

The self-assembly of low-molecular weight molecules into volume-spanning networks has been a subject of intense interest for the past two decades. These systems have been given many names, such as molecular gels, supramolecular gels, self-assembled fibril networks (SAFiN), or self-assembled networks.<sup>1,2</sup> The respective molecules have been termed *low* molecular weight gelators (LMWG).3-5 Regardless of their name, they all have in common the self-assembly of low molecular weight species (<1000 g/mol) into one-dimensional high aspect ratio aggregates, such as fibrils, needles, nanotubes webs, etc. Furthermore, they are typically dynamic systems that are characterized by incomplete crystallization and some form of equilibrium between free and self-assembled species.<sup>6,7</sup> The latter can adopt a variety of supramolecular structures. They often reflect a complex free energy landscape, which could result in thermodynamic or metastable (kinetically trapped) gels depending on solution parameters such as peptide concentration and ionic strength.8

Molecular gels are interesting from both a fundamental and applications point of view. For example, several diseases including Alzheimer's disease, Parkinson's disease, Huntington's disease, and prion-transmissible spongiform encephalopathies result from the self-assembly of peptides/proteins into fibrils. Thus, fundamental studies regarding the mechanisms and interactions that lead to the self-assembly of peptide/protein sequences are paramount to a better understanding of physiological fibril formation and possibly their prevention. Furthermore, there are numerous examples of molecular gels in industrial applications. For example, LMWGs

have been used in lubricants (found as early as 1700 BCE in chariot axles), <sup>15</sup> personal care products (uses dating back to 1550 BCE as topical wound treatments), <sup>16</sup> the food industry (thickeners such as plant waxes, lecithin, etc.), adhesives (glue sticks, pressure-sensitive adhesives, etc.), inks and printing. <sup>17–19</sup> For additional reading, the reader is referred to Weiss's excellent review of LMWG applications. <sup>20</sup> Potential biomedical applications of LMWGs include drug delivery and tissue engineering. <sup>2,82</sup>

As prevalent as LMWGs are in commercial applications, very little is understood regarding their mechanisms of self-assembly and network formation. From what is reported, most undergo microphase separation through nucleation phenomena rather than by spinodal decomposition.<sup>2</sup> Furthermore, a significant fraction of the molecules is in the form of a solid-phase continuous structure, also known as a three-dimensional (3D) volume-spanning fibrillar network. However, not all molecular gels have fibrillar elements, for example, nonfibrillar collagen gels. One undisputed feature of SAFiNs is that the storage modulus is always larger than the loss modulus over a large frequency range that spans several orders of magnitude.<sup>2</sup> The storage modulus G' of a sample is an indicator of the gel strength and reflects its elasticity, while the

Received: February 17, 2021 Revised: April 22, 2021 Published: June 16, 2021





**PDFelement** 

chemistry.

well as a better correlation between SAFiN properties and

loss modulus G'' is a measure of the ability of the network to rearrange and dissipate energy. This important point quantitatively distinguishes complex fluids from molecular gels. In many cases molecular gels are thermally reversible with their sol(ution) phase. However, there are some exceptions, such as the recently discovered gel phases of the cationic tripeptide glycylalanylglycine (GAG) in water/ethanol. It was found to self-assemble into a fibril network that, upon annealing these samples over several hours, melts into stable oligomers that are unable to refibrillate. Another commonality between LMWG is that the sol phase consists of individual gelator molecules or their small aggregates (oligomers) without forming a continuous network. Overall, a concise definition that captures the broad aspects of molecular gels is still missing.

Typical strategies for microgel formation involve heating a solid gelator and a liquid component until an apparent solution(sol) is achieved, followed by cooling below the solgel transition temperature. The rate of cooling and the solubility of the solute in the employed solvent dictates the nature of the gel. However, new formation strategies not using annealing are becoming more common in the literature. For example, alternative methods of using cosolvents <sup>23–25</sup> or pH switching to force the molecules to self-assemble have proven successful. <sup>26–31</sup>

One class of LMWG that is gaining considerable interest consists of short peptides (defined as m < 20, where m is the number of amino acids in the sequence). Potentially, they offer significant advantages in biomedical applications, such as biocompatibility and low cytotoxicity. Several reviews are available that summarize the extensive literature on SAFiN forming short and ultrashort peptides and delineate their usability for biotechnological and biomedical purposes.3-However, given the endless possibilities of amino acid sequences, we are only in the infancy of being able to predict peptide self-assembly a priori. Some researchers go as far to argue that all peptides and proteins are capable of selfassembly, it only requires the right conditions.<sup>32</sup> It therefore comes as no surprise that research in the field is predominately Edisonian in nature, with discoveries happening by chance.<sup>3</sup> The field is predominately focused on the chemical requirements for gel formation, with less regard for the underlying mechanism of and the structural requirements (fibril and network) for the formation of peptide gels.

This Perspective aims to summarize our current understanding of the whys and hows of short and ultrashort peptide gelation via the limited data sets that are available. More specifically, we will compare SAFiN-forming peptides in terms of their mechanism and kinetics of self-assembly as well as their structural properties, such as fibril length and thickness, and hierarchical structure of the fibril network. Moreover, we discuss the stability of such networks with regard to changes of concentration, pH, and temperature. Given the limited data set, the reader may notice that a large fraction of the literature is focused on di- and tripeptides. However, generalizations are made whenever possible. For example, we highlight the importance of amphiphilic sequences, hydrophobic interactions, and hydrogen bonding for the mechanism of selfassembly processes. It is worth mentioning that the methods and protocols discussed here are easily applicable to any arbitrating self-assembling system. Future work using and comparing these methods/protocols will hopefully lead to a better understanding of self-assembly in peptide systems, as

# A SHORT OVERVIEW OF MOLECULAR STRATEGIES FOR FORMING SAFINS

A complete list of SAFiN-forming peptides is outside the scope of this Perspective. Instead, we focus on the different strategies that have been successfully employed to synthesize SAFiN-forming peptides. For peptides with m>10, a common scheme of generating SAFiNs involves amphiphilicity, that is, the use of hydrophilic sequences/moieties to ensure the dissolution of the peptide and hydrophobic sequences/moieties to induce favorable interactions between dissolved peptides that lead to self-assembly. In the more recent category of ultrashort SAFiN-forming peptides (m<10), such as di- and tripeptides, the predominant strategy utilizes aromatic amino acid residues and end groups as well as amphiphilicity.

One successful strategy for synthesizing SAFiN-forming peptides with m>10 is to include repeating amino acid sequences that are amphiphilic. A prominent representative is the so-called MAX1 peptide and its derivatives synthesized and investigated by Schneider and co-workers (Figure 1).  $^{26,35,36}$ 

MAX1: VKVKVKVKVVDPPTKVKVKVKV-NH<sub>2</sub>

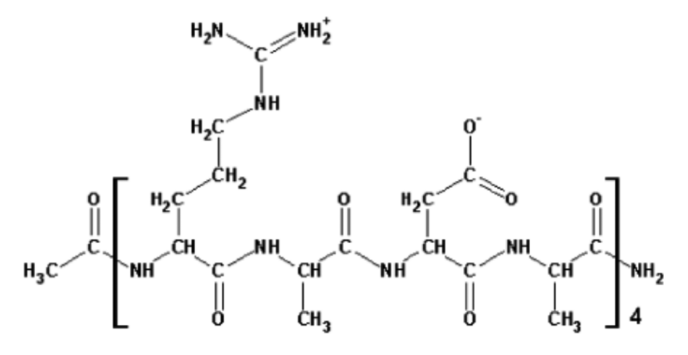


Figure 1. Structures of two amphiphilic peptides that are capable to self-assemble into SAFINs in appropriate solvent conditions. (upper) Folded structure of a MAX1 peptide. This peptide self-assembles either upon deprotonation of the lysine residues or by the addition of charge-neutralizing salts. Reprinted with permission from ref 26. Copyright 2002 American Chemical Society. (lower) The RADA peptide for which complementary charges facilitate self-assembly. Reprinted with permission from ref 34. Copyright 2008, Wiley & Sons.

The gelation capability of MAX1 arises from the sequences of hydrophilic lysine (K) and hydrophobic valine (V), repeats that are linked by a turn-forming V<sup>D</sup>PPT segment. The KV sequence provides amphiphilicity and  $\beta$ -strand propensity,<sup>37</sup> while the linking sequence facilitates the folding into a  $\beta$ -hairpin-like structure.<sup>38</sup> The self-assembly was shown to arise from hydrophobic interactions in the folded state and hydrogen bonding between solvated peptide groups.<sup>39</sup> The folding itself is triggered by the deprotonation of lysine groups,

**PDFelement** 

which reduces the repulsive interaction between strands or by adding a neutralizing amount of salt. <sup>26,36</sup> At sufficiently high concentrations, physical fibril entanglements and fibril branching lead to gelation. Another rather classical representative is the RADA peptide (R = arginine, A = alanine, D = aspartic acid) synthesized and investigated by Zhang and colleagues (Figure 1).<sup>27,40</sup> Here the hydrophilic side of the amphiphilic peptide is provided by an RD repeat, which carries a positive and a negative charge at neutral pH. This enables the formation of salt bridges between the charged end groups of R and D, which in addition to hydrophobic interactions between alanine side chains facilitate self-assembly.

Another strategy for producing amphiphilic biomolecules capable of forming SAFiNs is to react a hydrophilic or hydrophobic moiety with a peptide to form a hybrid molecule. More specifically, hydrophilic oligopeptides are linked to hydrophobic alkyl chains or hydrophilic groups are linked to hydrophobic peptides. The synthesis and application of these hybrid molecules have been pioneered by the Stupp group. 30,41 Most of them were used to produce cylindrical and ribbonlike nanofibers with high-aspect ratios. Zhang et al. reported a protocol aimed at producing highly anisotropic aligned monodomain gels of V<sub>3</sub>A<sub>3</sub>E<sub>3</sub>(CO<sub>2</sub>H) linked to a C<sub>16</sub> tail.

An alternative strategy to relying purely on hydrophobic interactions to induce self-assembly is to use functional groups to physically and chemically cross-link amphiphilic peptide molecules in solution. For example, multidomain peptides (MFPs), which were introduced by Hartgerink and co-workers, are typically composed of a block amino acid architecture, such as an ABA triblock architecture. 43,44 One successful example is MSP1, with the sequence of  $Ac-K_2-(SL)_6-K_2-NH_2$ , which is made amphiphilic by the use of leucine in the "B" block. The authors found that SAFiNs can be generated by chemical cross-linking via lysyl oxidase or physical cross-linking by the addition of salt to form ionic ligand bonds between charged lysine residues.

For some time it was believed that an oligopeptide must contain 10 or more amino acid residues in order to form SAFiNs. 45 However, this notion was challenged when ultrashort oligopepides were shown to form SAFiNs via a sequence containing aromatic amino acid residues. Classical examples are the islet amyloid peptide fragment NFGAIL and the amyloid  $\beta$  fragment A $\beta_{16-22}$ . The capability of aromatic residues to promote self-assembly and thus to reduce the critical length required for an oligopeptide to aggregate was demonstrated by the finding of Gazit and co-workers that phenylalanine dipeptides form very well-defined nanostructures like nanotubes, spheres, plates, and hydrogels. 4,48 This finding has triggered the development of many phenylalaninebased gelators, where the propensity for self-assembly and gelation of F-containing di- and tripeptides was enhanced by aromatic end groups attached to the N-terminal of the peptide (Fmoc: fluorenylmethyloxycarbonyl and Boc: tert-butyl decarbonate) (Figure 2). The computational study of Frederix et al. underscored the pivotal role of the aromatic amino acid residues F, Y, W and to a lesser extent H in facilitating the selfassembly of ultrashort oligopeptides. 33,49

Our activities in the field were triggered by the accidental observation that the unblocked tripeptides GAG and glycyl histidyl glycine (GHG) form uncharacteristically strong SAFiNs under controlled conditions. More specifically, GAG (Figure 2) forms SAFiNs in water/ethanol mixtures, <sup>24,25</sup> while GHG forms SAFiNs in water above pH 6.31,50 GAG highlights

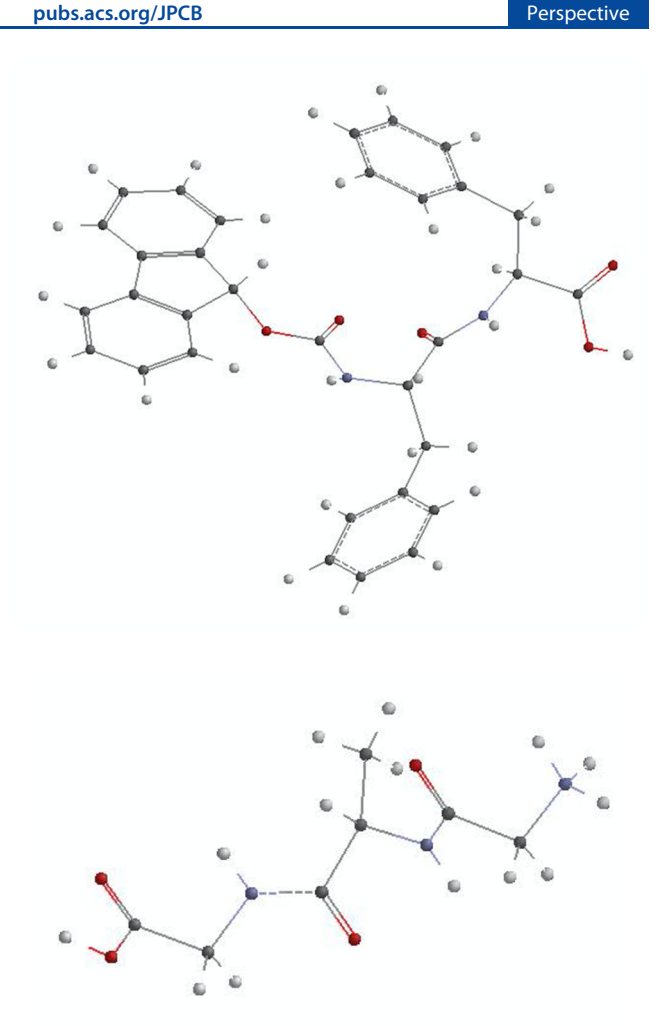


Figure 2. Two examples of ultrashort peptides that self-assemble into a gel-forming network in water or water-containing binary mixtures. (upper) Protonated FmocFF that self-assembles in response to a pH titration from alkaline pH or in water/DMSO mixtures. (lower) Cationic GAG, which gels in water/ethanol mixtures.

the fact that SAFiNs can form via amphiphilic tripeptides without aromatic side chains, while the gelation of GHG is currently thought to reflect the ability to form SAFiNs via aromatic side chains and hydrogen bonding between side chains and backbone groups. 31,51 Interestingly, histidine flanked by glycine residues in di- and tripeptides did not score high in propensity for self-assembly in the computational studies of Frederix et al., 33,49 despite the aromaticity of the imidazole ring in the deprotonated state. Compared to other peptide SAFiNs, GHG and GAG networks have peculiar properties with regard to the length and structure of fibrils, the strength of the formed gel, and its dependence on concentration and solution conditions. These properties are the subject of the following sections.

Note that, while amphiphilicity appears to be a key ingredient to ensure the formation of SAFiNs, very little is known regarding the mechanism and free energy landscape that favors self-assembly. Without such a fundamental understanding, it is not practical to imagine a connection between peptide sequence, propensity for self-assembly, and SAFiN mechanical properties. The computational work of Frederik and co-workers is certainly a step in the right

**PDFelement** 

direction, <sup>33,49</sup> but much more work and novel computational methods are needed to achieve SAFiNs by a chemical design approach. In the meantime, experimentalists should focus on techniques, such as spectroscopy, to characterize the self-assembled structure on the molecular scale and better understand which interactions are responsible for self-assembly. This is the subject of the following section.

# ■ SPECTROSCOPY AS AN IMPORTANT TOOL IN STUDYING SELF-ASSEMBLY MECHANISMS

Generally, there are three parameters that can be used to induce self-assembly, namely, pH, temperature, and ionic strength. In some cases, gelation can be triggered by the addition of a cosolvent. Depending on the peptide sequence, the relative importance of the three parameters varies significantly. Spectroscopic techniques are extremely useful for exploring the effect of different solution conditions on the interactions between individual molecules and their role in the self-assembly process. More specifically, IR, vibrational circular dichroism (VCD), and UV circular dichroism (UVCD) are very useful tools for probing the interactions that lead to self-assembly and specifics of the individual fibril structure. <sup>52–55</sup>

# CHARACTERIZING FIBRIL STRUCTURE IN PEPTIDE SAFINS

For most SAFiN-forming peptides discussed in this Perspective, spectroscopic evidence indicates that the fibrils are sheets with a  $\beta$ -sheet-like structure. The secondary structure is typically identified by UVCD and Fourier transform infrared (FTIR) measurements. UVCD spectra of  $\beta$ -sheets generally depict a strong positive maximum below 200 nm and a weaker negative maximum between 210 and 220 nm. For phenylalanine containing short oligopeptides UVCD is generally unsuitable for any secondary structure analysis owing to the large overlap of its absorption spectrum with the intrinsic absorption spectrum of the amino acid. As a consequence, electronic coupling between  $\pi \to \pi^*$  transitions of aromatic side chains and the peptide moiety has a significant influence on the UVCD spectrum.

FTIR spectroscopy is a more suitable technique for the determination of secondary structures but generally requires higher peptide concentrations.  $\beta$ -Sheets have a very clear spectroscopic fingerprint in the amide I region, where a strong excitonic coupling between amide I modes in adjacent strands leads to an apparent redshift of the band position from ca. 1650 cm<sup>-1</sup> to a position between 1610 and 1640 cm<sup>-1</sup>, depending on the extent an ideal sheet structure is deformed by twisting. 52,57,58 Antiparallel  $\beta$ -sheets give rise to another weak band between 1680 and 1700 cm<sup>-1</sup>. Generally, the amide I region of  $\beta$ -sheets shows some type of absorption continuum that covers the region between the low and high wavenumber band, which reflects the amide I dispersion caused by the above-mentioned excitonic coupling. 59

While several lines of evidence suggest that Fmoc-peptide derivatives self-assemble into  $\beta$ -sheets, Eckes et al. questioned the notion that the latter is the only possible secondary structure produced by the self-assembly of Fmoc peptides. They arrived at this conclusion by using IR spectroscopy and wide-angle X-ray scattering (WAXS) measurements to compare the fibrils produced by the self-assembly of Fmoc-AA and Fmoc-A-Lac, where Lac denotes lactic acid. Despite the fact that the Lac moiety of Fmoc-A-Lac is incapable of

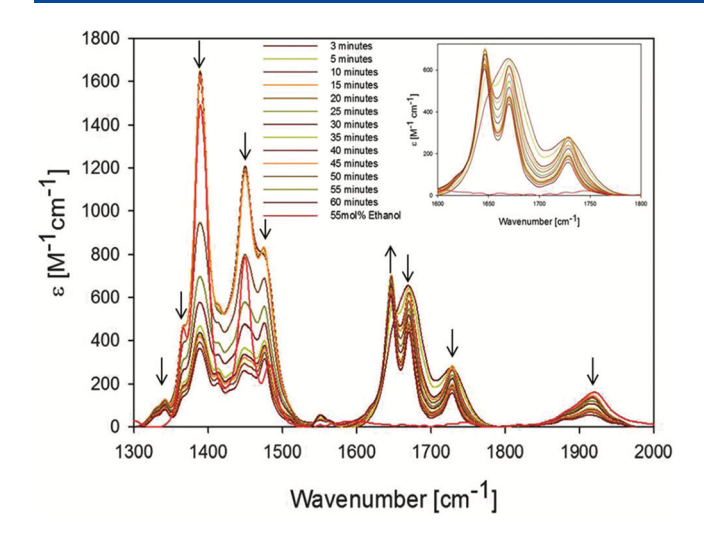
forming hydrogen bonds, WAXS patterns of both dried peptide films showed very similar patterns and indicated  $\beta$ -sheet structures. The authors concluded from their study that hydrogen bonding might not play a significant role in the self-assembly of low molecular weight peptides such as Fmocpeptide derivatives. Moreover, molecular dynamics simulations suggest that Fmoc-A-Lac adopts a mixture of polyproline II (for alanine) and right-handed helical (Lac) rather than one of the canonical  $\beta$ -strand conformations.

Recently, more evidence has been added for the notion that  $\beta$ -sheets are a necessary ingredient of peptide fibrils. Tantakitti et al. investigated the energy landscape governing the selfassembly of hybrid peptide amphiphiles by covalently bonding a V<sub>3</sub>A<sub>3</sub>K<sub>3</sub> peptide to a 16-carbon alkyl chain.<sup>8</sup> At a low ionic strength, the repulsion between the lysine residues produced short monodisperse fibrils, which thermodynamically represented a metastable state. The corresponding peptide structure was identified as a random coil via UVCD spectra. However, the negative amplitude of the latter and the three alanine residues in the oligopeptide fragment suggests a statistical coil with a significant sampling of polyproline II conformations.<sup>61</sup> In the presence of a high concentration of salt, the latter screens the positive charges on the lysine side chains leading to the formation of longer  $\beta$ -sheet fibrils. A similar relationship between fiber length and structure was recently reported for FmocFF. While the fibrils in the gel phase (in aqueous solution and in water/dimethyl sulfoxide (DMSO) mixtures) clearly exhibit  $\beta$ -sheet character, the peptide forms short, amorphous fibrils in DMSO in the centi- and submolar region of the peptide concentration.<sup>22</sup> A rather novel sheet structure has recently been reported by Bera et al. who found that the unblocked tripeptide PFF self-assembles into helical sheets that form a supramolecular structure by interactions between interfaces formed by phenylalanine residues.84

Lately, we found that cationic GAG SAFiNs in water/ ethanol mixtures are not formed by canonical  $\beta$ -sheet structures irrespective of peptide concentration and ethanol fraction. More specifically, we found that the spectral dispersion in the amide I region for cationic GAG in water contains two bands at ca. 1649 and 1670 cm<sup>-1</sup>. These bands are unmistakably assignable to excitonically coupled C- and Nterminal amide I vibrations. This doublet collapses into a nearly single amide I band at 1669 cm<sup>-1</sup> above an ethanol fraction of 40 mol %.63 When the 200 mM GAG in 55 mol % ethanol/45 mol % water self-assembles to form a gel, this band splits into comparatively sharp bands at 1646 and 1670 cm<sup>-1</sup> (Figure 3), which are clearly distinct from any reported  $\beta$ -sheet band profile of amide I.<sup>25</sup> At room temperature the amide I VCD shows a strongly enhanced negative couplet, which is indicative of left-handed chirality (Figure 3, phase II of two observed gel phases). An even stronger positive couplet was observed for phase I (10 °C), which indicates that the fibrils in the two phases exhibit opposite chirality.

Apparently, the self-assembly of GAG requires some type of sheet formation but not a traditional  $\beta$ -sheet structure. Our experimental observations are supported by density functional theory (DFT) calculations of GAG oligomers in implicit water and ethanol, which show that the self-assembly of this peptide is indeed possible without an underlying  $\beta$ -sheet structure. Ilawe at al. showed that a parallel arrangement of GAG peptides leads to a somewhat disordered sheet structure where individual strands adopt polyproline II,  $\beta$ -strand, and  $\gamma$ -turn structures. <sup>64</sup> In an antiparallel arrangement, GAG was found to

**PDFelement** 



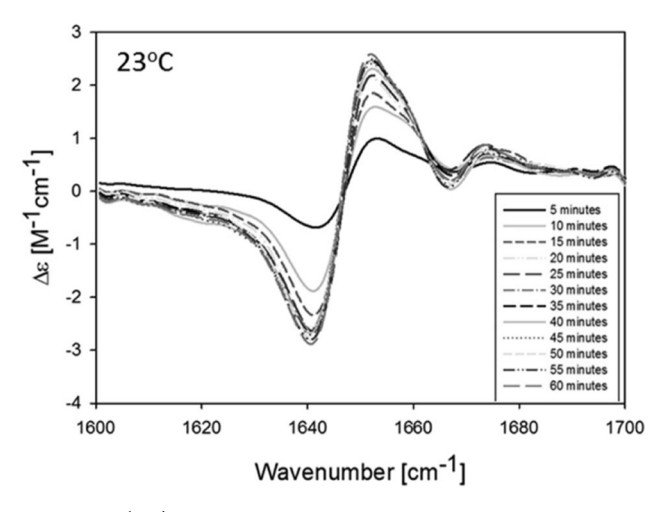


Figure 3. (left) FTIR spectra of 220 mM GAG in 55 mol % d-ethanol/45 mol %  $D_2O$  measured at 10 °C with an inset of the amide I region. The red line depicts the spectrum of the solvent mixture without peptide. (right) Amide I' region of the VCD spectra of 220 mM GAG in 55 mol % d-ethanol/45 mol %  $D_2O$  measured at different times after incubation at the indicated temperatures. The arrows indicate the changes of the spectra over time. Reprinted with permission from ref 25. Copyright 2016 Royal Society of Chemistry.

form a highly bent  $\beta$ -strand structure. Interstrand hydrogen bonding is complicated because it involves peptide and terminal groups. The simulated IR and VCD spectra bear a significant similarity with the experimental band profiles (Figure 4 for phase II). Interestingly, recently reported WAXS data of GAG gels would be fully consistent with a canonical  $\beta$ -sheet structure. Hence, our data underscore the notion that sheets with different secondary structure content might exhibit a similar spacing between the incorporated strands and sheets.  $^{60}$ 

Recently, we measured the IR spectrum of the gel phase formed by 175 mM GHG upon deprotonation of the imidazole side chain. The amide I region seems to resemble a superposition of  $\beta$ -sheet and monomer spectrum. However, a closer inspection of the spectral composition revealed that this might be an oversimplification in that the amide I profile is likely to contain at least four sub-bands in the region between 1630 and 1690 cm<sup>-1</sup>. We are in the process of constructing a structural model that simultaneously explains the amide I

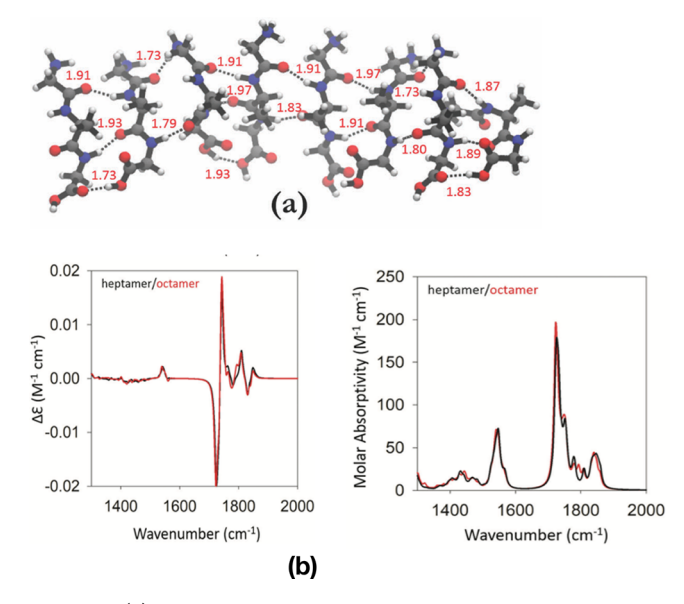


Figure 4. (a) Structure and hydrogen-bonding pattern of the octamer with parallel GAG orientation obtained from geometry optimization. (b) Calculated VCD (left) and IR spectra (right) of a geometry-optimized GAG heptamer (black) and octamer (red) with a parallel strand orientation in implicit water. Reprinted with permission from ref 64. Copyright 2018 Royal Society of Chemistry.

profile and reported WAXS data. Currently, we wonder whether GxG peptides with the capability to self-assemble into gels (x represents nonglycine guest residues) do have in common that the respective fibrils do not resemble classical  $\beta$ -sheet structures.

We have already mentioned the importance of hydrophobic interactions as a prominent force in peptide self-assembly.  $^{39,66}$  However, it is not clear why the self-assembly prefers a rod or fibril confirmation. One hypothesis is that peptide fibrils are generally formed by the self-assembly of sheets. For example, Aggeli et al. proposed that fibers are formed from elementary peptide building blocks that adopt a rod-like  $\beta$ -strand conformation. These rods assemble into helically twisted tapes via stacking. Hydrophobic interactions promote the formation of double tapes (ribbons), which further assemble into fibrils. The model of Aggeli et al. argues that the formation of well-defined fibrils requires the tapes to be twisted. While this model does explain much of the literature, there are some exceptions, which suggest that there may be more than one mechanism for peptide fibril self-assembly.

# ■ THERMAL STABILITY OF PEPTIDE SAFINS

It is astonishing that systematic investigations of the thermal stability and reversibility of peptide SAFiNs via spectroscopy are rather limited in number, despite their potential importance in developing and validating thermodynamic descriptions of the self-assembled peptide structure. For example, Ye et al. measured the UVCD spectrum of 100  $\mu$ M RADA16-I as a function of temperature between 25 and 80 °C at pH 4.<sup>27</sup> The data suggest a  $\beta$ -strand  $\rightarrow$  statistical coil transition with increasing temperature. The reported spectra seem to suggest a melting temperature of ca. 70 °C. Another example is the work of Pochan et al., who used UVCD spectroscopy to investigate the melting of three MAX peptides termed MAX1 (Figure 1), MAX2, and MAX3.<sup>68</sup> MAX2 and MAX3 differ from the above introduced MAX1 by replacing

**PDFelement** 

the valines in the fourth and sixth VK repeat by threonine. The spectroscopy clearly shows that this leads to a significant stabilization of  $\beta$ -sheet assemblies. MAX1 melts at ~30 °C, MAX2 with a single V  $\rightarrow$  T displacement at 40 °C, and MAX3 with two substitutions above 60 °C (Figure 5). Since UVCD

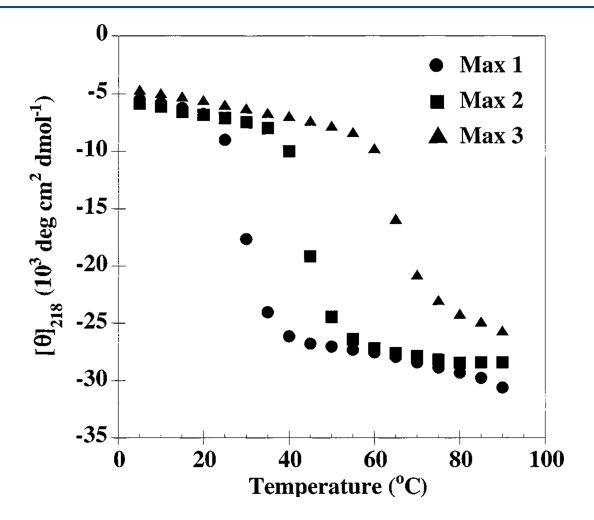


Figure 5. Temperature-dependent ellipticity of the indicated MAX peptides measured at 218 nm plotted as a function of temperature. The spectra were recorded with a 150  $\mu M$  peptide solution at pH 9. Reprinted with permission from ref 68. Copyright 2003 American Chemical Society.

probes the melting of individual fibrils it is thinkable that the loss of rheological properties starts at lower temperatures. The relationship between the melting of fibrils and the gel will be discussed in a later section.

The melting of GAG gels in water-ethanol depends heavily on peptide concentration and the ethanol fraction of the water-ethanol mixture. Figure 6 shows the UVCD signal of GAG at 221 nm as a function of temperature between 20 and 70 °C. At this wavelength a comparatively intense positive maximum appears in the CD spectrum of the gel phase.<sup>25</sup> With increasing temperature, the respective dichroism approaches zero or even a slightly negative value, which indicates a dissolution/melting of the fibrils. Each melting curve was analyzed with a two-state model to determine the melting temperature as well as the enthalpic and entropic differences between fibril and sol phases.<sup>69</sup> The melting temperature was found to increase moderately with peptide concentration but more significantly with ethanol fraction from 0.5 to 0.7 mol %. This reflects the decreased solubility of the GAG in solvents with a high ethanol fraction. Below, we directly compare the peptide concentration and ethanol fraction dependence of the fibril melting temperature with that of the network softening temperature obtained from rheological measurements.

Spectroscopy is also essential in understanding whether a self-assembled structure is thermodynamically stable. For example, thermal annealing experiments revealed that a GAG fibril self-assembly is not thermally reversible. More specifically, heating 200 µM GAG in 55 mol % ethanol/45 mol % water to 50 °C for a prolonged time leads to an irreversible loss of self-assembled fibrils. While the respective IR spectrum suggests that the underlying structure is disordered, the very unusual UV absorption spectrum and the still partially enhanced amide I' VCD signal indicate some sort of amorphous aggregates with some strong electronic interactions

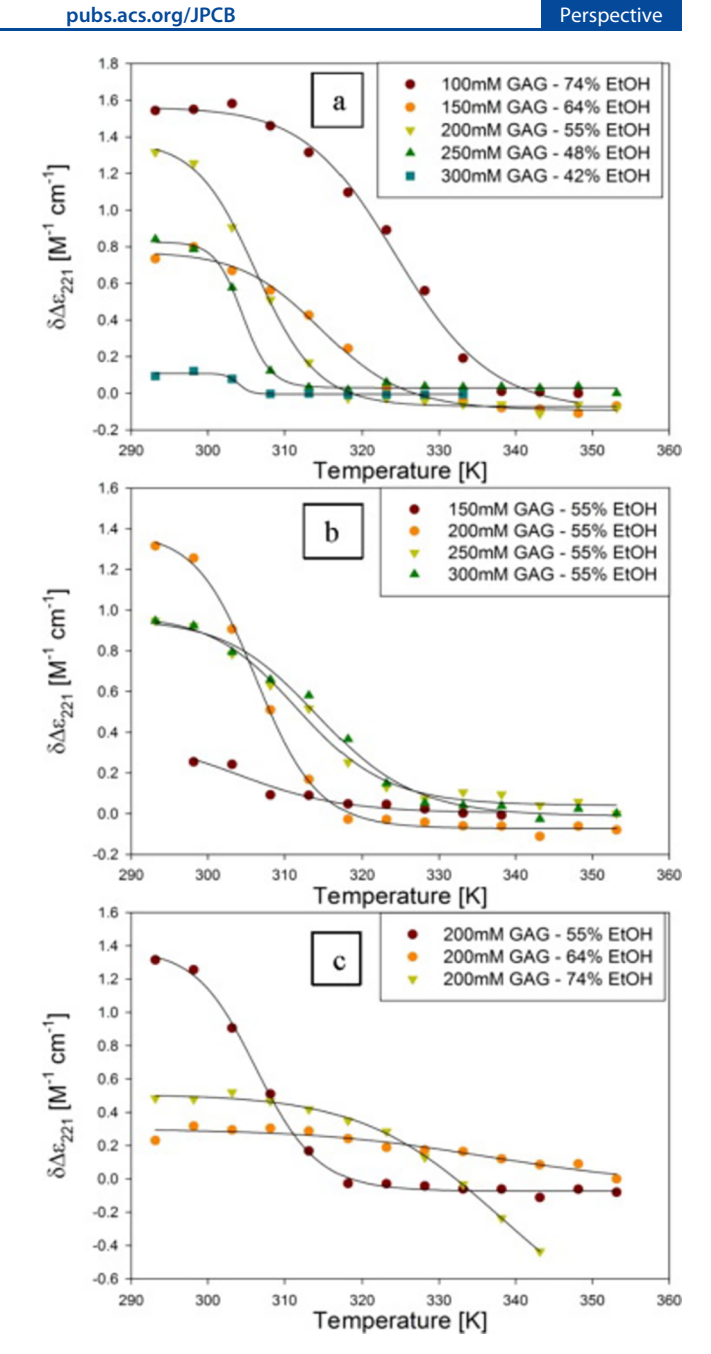


Figure 6. Melting curves of individual GAG fibrils probed by plotting the ellipticity at 221 nm as a function of temperature for the indicated peptide concentrations and ethanol fractions. As shown in Farrell et al. 25 the UVCD spectra of GAG gels show a peculiar positive maximum at this wavelength, which disappears upon melting. The solid lines result from the fits of a two-state thermodynamic model to the experimental data, which is described by DiGuiseppi et al. Reprinted with permission from ref 69. Copyright 2020 Elsevier.

between excited electronic states.<sup>21</sup> The results of these annealing experiments underscore the relevance of intermediate states in the stability and thermal reversibility of SAFiNs.

However, studies lacking a detailed spectroscopic analysis unfortunately leave many more questions than answers. For example, Orbach et al. measured the weight loss of several gels formed by a variety of Fmoc di- and tetrapeptide.<sup>23</sup> It is not clear whether the data reflect gel melting or the dissociation of fibrils. The transition temperatures of all peptides investigated, which included FmocFF investigated, are very high, that is,

**PDFelement** 

above 100  $^{\circ}$ C. A more thorough thermodynamic analysis of the underlying physics of this exceptional stability of the gel phase is outstanding and would be highly desirable.

Generally, we would like to emphasize that knowledge of the thermal stability of gels is of utmost importance for their biotechnological applicability, since the average body temperature is 37 °C. Moreover, an understanding of the fibrillar/gel state itself requires some information about the enthalpy and entropy of formation. Measuring and analyzing the temperature dependence of spectroscopic indicators generally yields information about the stability of fibrils and sheets. Furthermore, calorimetry can be used to quantify the heats of formation. The stability of the gel network can be explored via rheology as a function of temperature (vide infra). Any of these approaches should be pursued more systematically in the future to connect molecular structure with self-assembly mechanisms.

#### PH EFFECTS ON PEPTIDE SAFINS

The pH dependence of SAFiNs has been studied somewhat more regularly. This is not surprising, since SAFiNs contain several residues with ionizable side chains. If a single charge dominates the peptide sequence, repulsive interactions typically prevent self-assembly, while complementary charges facilitate it. In the case of the dominance of either positive or negative charges, the decrease or increase of pH can cause their neutralization and thus enable self-assembly. 26,27 The latter scenario applies to MAX1 peptides and their derivatives. As shown in Figure 1, this oligopeptide contains mostly lysine side chains on its hydrophilic side. If all these residues are protonated electrostatic repulsion stabilizes the monomeric statistical coil state of the peptide. The pK value of lysine is 10.5, but Schneider and co-workers observed self-assembly and gel formation at pH 9.26 This observation suggests a lower effective pK value of the involved lysine groups. This has two reasons. First, repulsive interactions between charged lysine residues can destabilize the protonated state. Second, the formation of peptide fibrils and the subsequent gelation stabilize the neutral state of the residue.

For some peptides the protonation of side chains does cause changes of the state of self-assembly rather than a clear-cut transition between a gel and a monomeric sol phase. One example is RATEA16 (CH<sub>3</sub>CONH-RATARAEARATARAEA-CONH<sub>2</sub>).<sup>70</sup> At neutral pH the arginine residues are positively charged, and the glutamic acid residues are negatively charged. An attractive electrostatic interaction and salt bridge formation between these groups together with a hydrophobic interaction between alanine and threonine residues facilitate the selfassembly into fibrils with lengths on a 100-200 nm scale. At very acidic (3.5) and alkaline pH (12.5) self-assembly still takes place, but repulsive interactions and limited fibril length prevent gel formation at an acidic pH, while hydrophobic peptide-solvent interactions cause a precipitation. Similarly to RATEA 16, the more prominent amphiphilic peptide RADA shows a complicated dependence on pH. At very acidic pH (1.0) below the effective pK of the aspartic acid residues 100  $\mu M$  of the peptide still forms a sample spanning the network of fibrils, in spite of the positive charges of the arginine residues. Only with a very alkaline pH of 13, the now predominantly negatively charged peptides form small-size globular aggregates.70

For both cases discussed above pH changes can be utilized as a trigger for gelation, but in none of the cases it involves a

clear transition between monomers on one side and peptide fibrils in the gel phase on the other side. The situation is similarly complicated for the seemingly simple dipeptides with Fmoc end groups. Figure 2 shows the structure of Fmoc-FF-OH, the most prominent representative of this group. While Fmoc promotes aggregation, the overall propensity for selfassembly depends on the aromaticity of the amino acid residues. Generally, only the C-terminal carboxylate group carries a charge that could inhibit self-assembly. There are basically two protocols by which the gelation of FmocFF is achieved. One starts with the peptide dissolved in DMSO. Gelation is subsequently achieved by adding water as a cosolvent to the sample, which promotes  $\pi\pi$ -type aggregation of Fmoc and phenylalanine side chains. Alternatively, one would dissolve the peptide in water at an alkaline pH and titrate the sample into the acidic region to ensure the protonation of the C-terminal. However, titration curves reported by Tang et al. reveal that the protonation curves of this seemingly simple peptide depend on peptide concentration in a complex way (Figure 7). At low concentrations

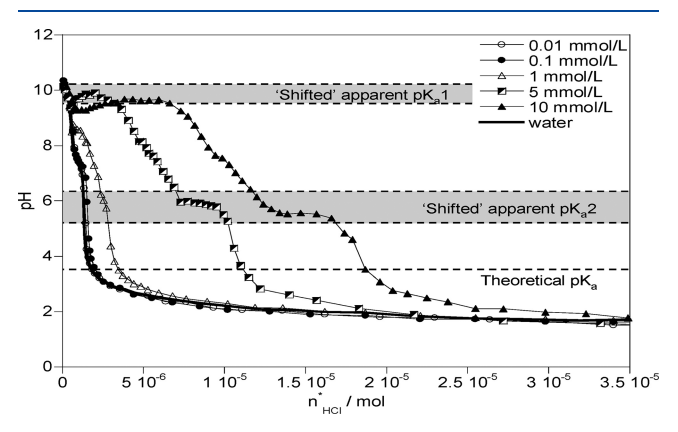


**Figure 7.** pH of Fmoc-FF in water vs moles of added HCl measured with 0.01, 0.1, 1, 5, and 10 mM peptide concentration. Reprinted with permission form ref 71. Copyright 2011 American Chemical Society.

(0.01 mM) the titration curve reflects the expected pK of the terminal COOH group of 3.5. However, when the peptide concentration is increased to 10 mM, the curve becomes first bi- and eventually triphasic. The authors identified two so-called shifted pK values at 10 and ca. 5.8. Above pH 10, spectroscopy revealed a mixture of monomers and a few fibrils, very similar to what was recently reported for FmocFF in DMSO. At pH 9, the sample forms a weak, self-supporting hydrogel. At pH 6.8 just above the second pK the solution became turbid and viscous. Generally, the results of Tang et al. suggest that different types of peptide assemblies lead to different shifts of the apparent pK value of the C-terminal carboxylate group. While interesting from a physical chemistry point of view, this complex behavior somewhat limits the use of pH as a sol  $\rightarrow$  gel switch.

None of the above peptides show the clear-cut phase transition between sol and gel phases, which one would like to see if one wants to use changes of pH as a trigger for gelation. Moreover, most of the effective pK values reported are not even close to the physiological region. Generally, one would expect histidine to be a more appropriate candidate in this regard. However, there are relatively few studies of histidine-containing gelators. Moyer et al. showed that a heptahistidine peptide linked to two aliphatic chains on its N- and C-terminal

**PDFelement** 

sides exhibits a structural transition between pH 6 and 6.5.30 At a pH above this transition region they observed a sample spanning network of cylinders if they used oligo(ethylene glycol) as a tail.

Recently, our group found that the unblocked GHG peptide self-assembles in a gel-forming sample spanning network above pH 6.31,50 Figure 8 shows the phase diagram for GHG with

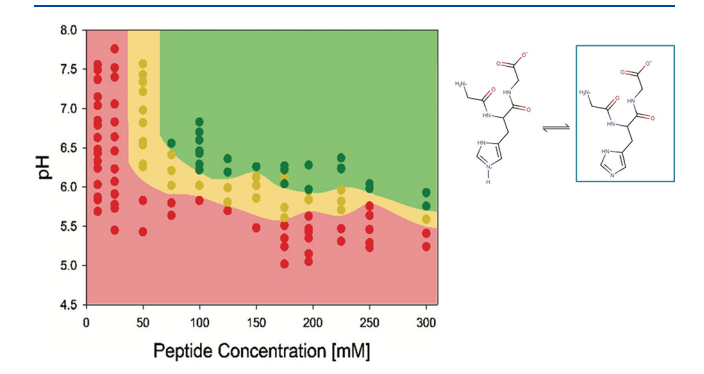


Figure 8. Phase diagram of GHG in water with respect to peptide concentration and pH. Samples were characterized visually as showing no visible large-scale peptide fibrils (red dots), partial self-assembly (yellow spots), and sample spanning fibrils (green dots). The background was added as a visual guide for the three phases. (inset) The structures of protonated and deprotonated GHG. Taken from ref 31 and modified.

respect to peptide concentration and pH. The critical pH for self-assembly decreases with peptide concentration, indicating that the deprotonated state is stabilized in the gel phase. There is a small transition region between the sol and the gel phases in which GHG already self-assembles without forming a sample spanning network. Compared with the pH dependencies discussed above the pH-induced triggering of GHG selfassembly seems to be a very well-defined process with an effective pK close to physiological pH.

#### RHEOLOGY OF PEPTIDE HYDROGELS

Before fibrillization, a solution of SAFiNs is a Newtonian fluid with a viscosity very close to that of the solvent, for example, water for hydrogels. However, as the peptides begin to selfassemble and create connections that span the volume of the

sample, a non-Newtonian viscoelastic response grows with time, until a steady-state network is achieved. The rheological properties of the network are typically probed in the linear viscoelastic regime using a small amplitude oscillatory shear (SAOS). The measurement is reported in terms of the elastic (G') and viscous (G'') moduli, which give an indication of the type, strength, and relaxation time scales of the gel. Much of the microgel literature indicates a gel by using an inversion test, which defines a gel as the inability of a solution to flow down the side of an inverted vial. Unfortunately, this definition is neither specific to gels nor provides any information about the network microstructure. For example, a solution of poly(vinyl alcohol) (PVA) and borate would satisfy this definition, but it is not, by any rheological definition, a gel, as it shows purely viscous tendencies at long times (low frequency). Although no concise definition of self-assembled peptide gels yet exists, one undisputed fact is that a molecular gel has a storage (elastic) modulus greater than the loss (viscous) modulus over a large frequency range, typically  $0.01 \le \omega$ , rad/s  $\le 100$ . Note that the gel strength is typically reported as the individual complex modulus,  $G^* = \sqrt{{G'}^2 + {G''}^2}$ , and/or the tangent of the phase angle tan  $\delta$ . This definition of a gel is illustrated in Figure 9, which shows the frequency dependence of moduli G' and G''for GAG in a 55 mol % ethanol solution. The data in Figure 9B further show that an annealing of GAG gels over a very short time interval (2-5 min) restores the respective gel phases but with lower G', G'', and tan  $\delta$  values.

Figure 10 displays rheological moduli of MAX1 in a salt solution at neutral pH. The gel strength G' is more than an order of magnitude lower than that of the GAG gel phases. This and the lower tan  $\delta$  values indicate a more elastic gel. It is evident that peptide concentration, formation temperature, and ionic strength strongly influence the network macrostructure and thus the modulus. The gel kinetics shown in Figure 10B reveals the role of NaCl in promoting a higher gel strength (larger G') and faster gel formation.<sup>72</sup>

The modulus of SAFiNs is controlled by both fiber properties and the overall macrostructure of assembled fibrils. Important fiber properties are the average fiber thickness and fiber modulus, which is expected to depend on intermolecular interactions. The stronger the intermolecular interactions, the higher the fiber modulus. The average fiber thickness seems to

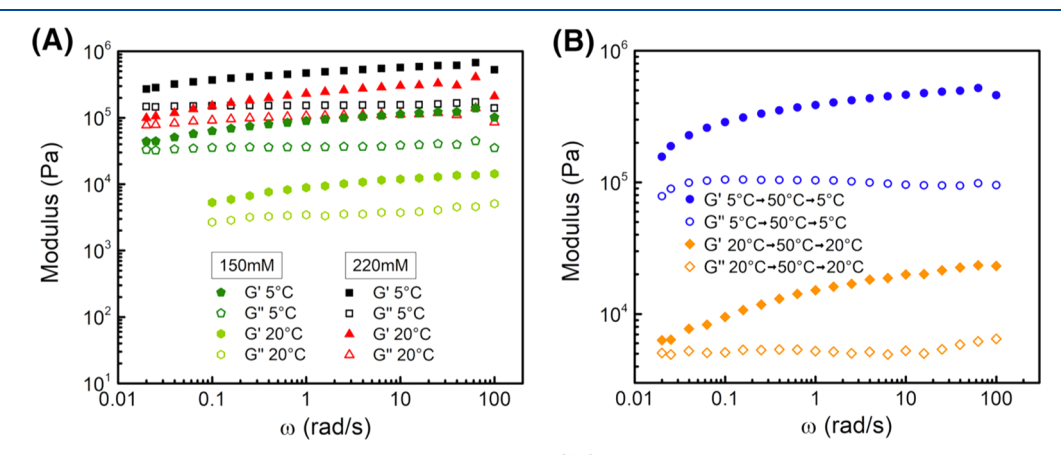
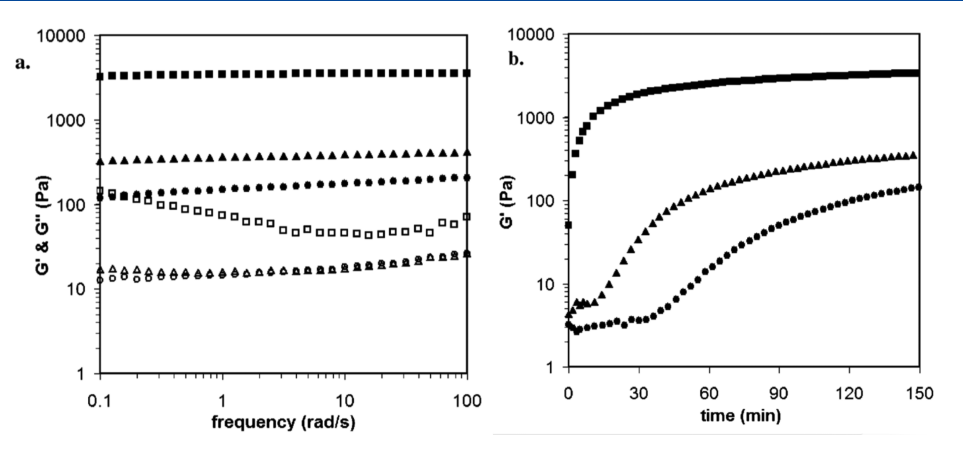


Figure 9. (A) Dynamic frequency sweep of the storage and loss modulus of 150 and 200 mM cationic GAG in 55 mol % ethanol/45 mol % water measured at the indicated temperatures. (B) Dynamic frequency sweep of the storage modulus of 200 mM cationic GAG in 55 mol % ethanol/45 mol % water measured after the indicated annealing cycle. Reprinted with permission from ref 65. Copyright 2021 Wiley & Sons.



**Figure 10.** (a) Dynamic frequency sweep (5% strain) of 2 wt % MAX1, pH 7.4 solution with 20 mM (G',  $\blacksquare$ ; G'',  $\bigcirc$ ), 150 mM (G',  $\blacktriangle$ ; G'',  $\triangle$ ), and 400 mM (G',  $\blacksquare$ ; G'',  $\square$ e) NaCl at 20 °C. (b) Dynamic time sweep (1% strain, 6 rad/s) of a 2 wt % Max1 solution with 20 mM ( $\blacksquare$ ), 150 mM ( $\blacksquare$ ) and 400 mM NaCl ( $\blacksquare$ ). Reprinted with permission from ref 72. Copyright 2015 American Chemical Society.

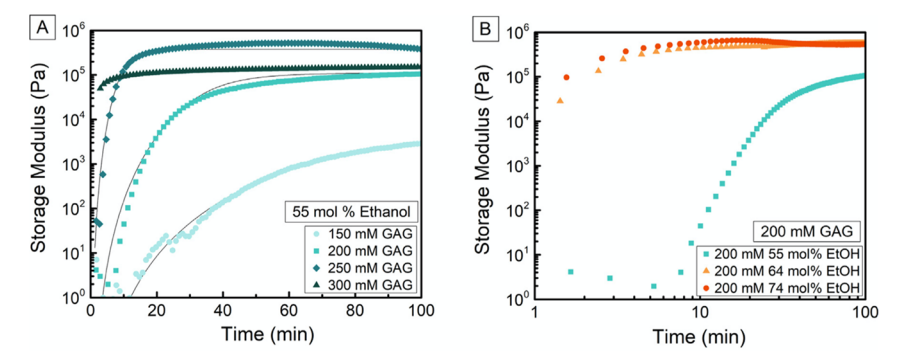


Figure 11. Kinetic traces of the storage modulus for the network formation (A) of cationic GAG (A) in 55 mol % ethanol/45 mol % water at different peptide concentrations and (B) of 200 mM GAG in the indicated water—ethanol mixtures. The solid lines in (A) result from a fit of an inverse power law to the experimental data. Reprinted from ref 74 with permission. Copyright 2020 Elsevier.

be related to intermolecular interactions; however, more work is needed to quantify this relationship. The macrostructure of the fibril network depends on the type of cross-links (physical or chemical), the number cross-links per fibril, and the overall organization of fibrils at long length scales, for example, network homogeneity. The degree of cross-linking and the organization of fibrils is poorly understood, although there is evidence that the number of nuclei and rate of formation play an important role. Y3,74 Such correlations will require a detailed rheological study of multiple peptide hydrogels under various conditions, which is severely lacking in the current literature.

It is well-established that the SAFiN modulus is an important property for biomedical applications, such as in tissue engineering, or drug delivery. However, for the most part the broad category of hydrogels possesses poor mechanical properties when compared to that of human tissues. One exception is polymer hydrogels made from freeze—thawing poly(vinyl alcohol), which can achieve tensile moduli similar to that of articular cartilage, that is,  $G^* \approx 1$  MPa. To For comparison, typical peptide hydrogels, such as MAX1 and Fmoc-peptides, have shear moduli on the order of 1–10 kPa at best. An exception are the peptide hydrogels recently produced using GAG and GHG, which have shear moduli comparable to that of PVA gels, that is, 0.1–1 MPa (Figures 9 and 10).  $^{31,74}$ 

Note that tensile properties for peptide hydrogels are almost completely absent from the literature. Two important goals for the future of peptide hydrogel research will be to measure nonlinear tensile and compressive properties to compare with biologically relevant mechanical properties and establish correlations between network mechanical properties and the chemical functionality of the peptide.

It is understood that the self-assembly process strongly influences the network macrostructure and, thus, the mechanical properties of the hydrogel. Kinetic rheological studies are useful in understanding the fundamentals of how solution parameters influence network formation and fibril organization, as clearly revealed by our own studies of the effect of peptide concentration, solvent ratios, pH, and temperature on the effect of network formation of GAG and GHG. 31,69,74 Figures 10 and 11 exemplify the rate of network formation on the concentration of peptide. Generally, the rate of network formation is a monotonic function of the concentration of peptides. However, this is not always the case. One might expect that, as the number of fibrils increases, the network becomes denser, the interstitial network pores become smaller, and the network modulus becomes higher. This has indeed been observed for some SAFiN such as RATEA 16.70 However, this expectation assumes that the network forms homogeneously in solution at all concentrations. At relatively low peptide concentrations, we do in fact observe an increase in the network modulus with increasing peptide concentration for cationic GAG gels, as shown in Figure 11. However, at very high concentrations of this peptide (400 mM), the self-assembly process is very rapid, which based on light microscopy images (Figure 12) appears to induce an

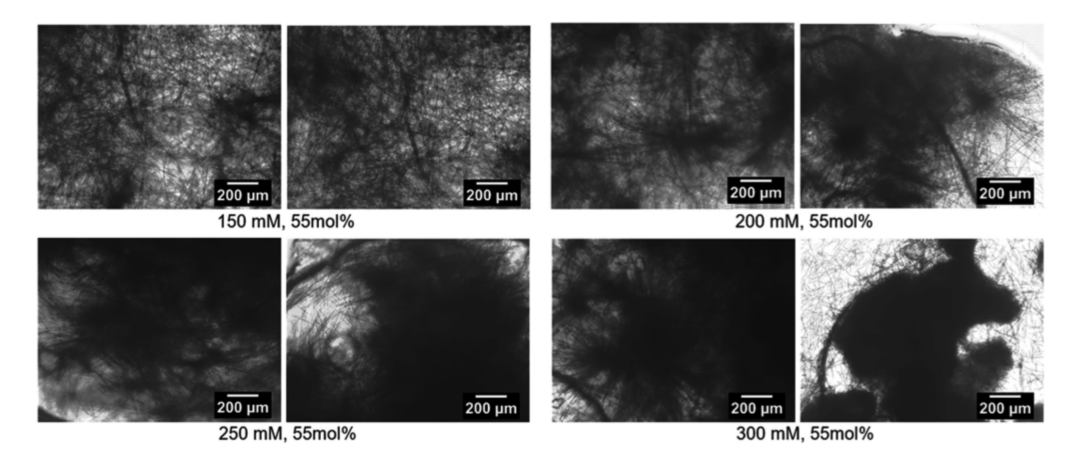


**Figure 12.** Optical microscope images of fibril macrostructure of gels formed with the indicated concentration of GAG in 55 mol % ethanol/45 mol % water. Reprinted from ref 74 with permission. Copyright 2020 Elsevier.

inhomogeneous network formation with dense domains of fibrils separated by sparse fibril domains.<sup>74</sup> This heterogeneity results in a reduced SAFiN modulus.<sup>3</sup>

Rheology is also a very useful tool to study the stability of peptide fibrils to external stimuli, such as pH, temperature, and dilution, especially when coupled with spectroscopy. Figure 13

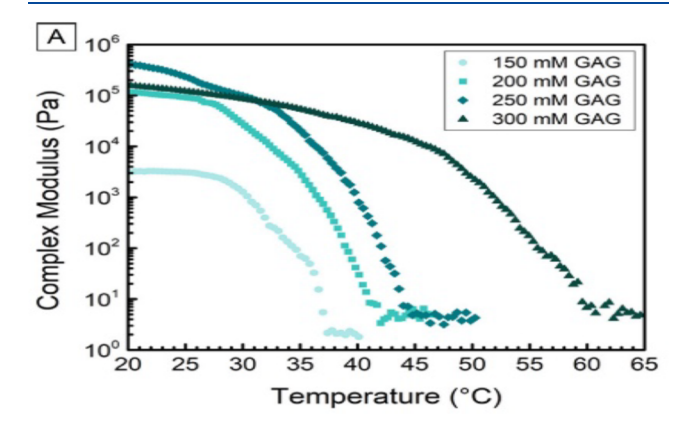


**Figure 13.** Dynamic temperature sweeps for solutions of GAG in 55 mol % ethanol/45 mol % water at four concentrations. These figures indicate that self-assembled fibrils are dissolved at increased temperatures, which reduces the bulk shear modulus. Reprinted from ref 74 with permission. Copyright 2020 Elsevier.

depicts the moduli of GAG fibrils as a function of temperature. In both cases, the results indicate that, at elevated temperatures, the number of fibrils is significantly reduced, which causes a lowering of the network modulus. At present most peptide hydrogel mechanical properties are reduced at elevated temperatures due to the increased solubility of the self-assembled structures. However, the thermal stability as probed by rheology is only specific to the network under investigation.

The combination of rheology and spectroscopy allows for a decoupling of the fibril melting and network softening. The former is expected to be independent of network structure, while the latter is explicitly dependent on the homogeneity of the network. For example, the phase diagram in Figure 14 shows the concentration and ethanol fraction dependence of the softening temperature inferred from measuring the temperature dependence of the storage modulus. The left phase diagram shows the concentration and pH dependence of the melting of individual fibrils. Generally, the softening temperature is lower than the melting point of individual fibrils. Furthermore, the softening dependence is less monotonic compared with the behavior of the melting temperature. However, DiGuiseppi et al. still observed a rather significant correlation between melting and softening temperature with a correlation coefficient of  $R^2 = 0.89$ .

The work described in this paragraph reveals the necessity to study the thermal stability of gels with different techniques so that the melting of fibrils and other self-assembled structures

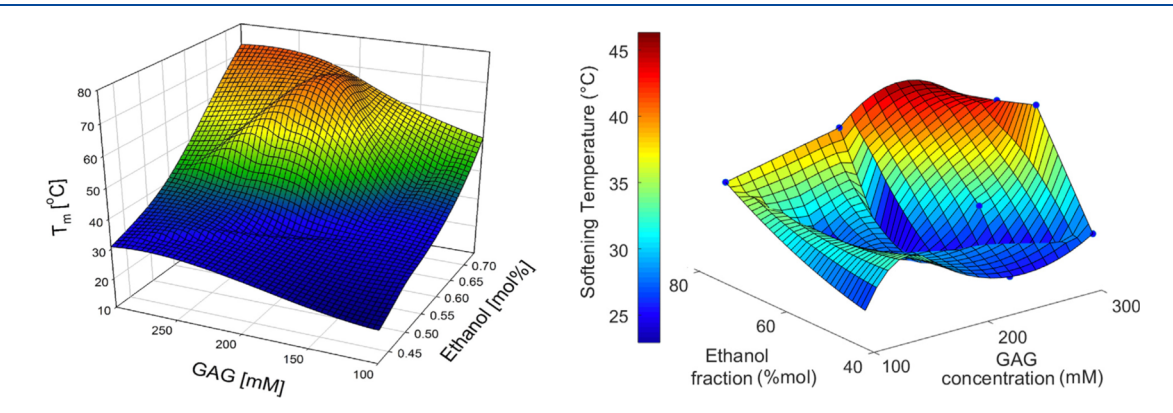


**Figure 14.** Phase diagrams for GAG/water/ethanol samples in three dimensions spanned by coordinates representing peptide concentration, ethanol fraction, and the melting temperature of the fibrillar state (left) as well as the softening temperature of the gel phase (right). Taken from refs 69 and 74 with permission. Copyright 2020 Elsevier.

Perspective

can be distinguished from and related to the gel stability probed by rheology. Such combined measurements are rare in the literature.

The Journal of Physical Chemistry B

In assessing the usefulness of a given peptide hydrogel formulation for biomedical applications, one must consider mechanical properties at body temperature (~37 °C). Future studies should make a point to measure the effect of temperature on network stability so that different hydrogels can be compared and assessed. For pH-dependent gelation processes it is important to fully characterize the sol  $\rightarrow$  gel transitions and to identify gelators for which this switch occurs at or close to the physiological pH. In the subsequent section we discuss the kinetics of fibrilization and gelation, via combined spectroscopy and rheology, to quantify gelation mechanisms and properties.

# KINETICS OF FIBRILIZATION AND GELATION—COMBINING RHEOLOGY AND **SPECTROSCOPY**

A survey of the literature regarding SAFiN peptides reveals a lack of a thorough kinetic analysis of the respective selfassembly and gelation processes. In many cases, the authors report the result of kinetic measurements without a detailed kinetic analysis. However, if we are ever to establish structureproperty relationships in peptide hydrogels, we must focus on the analysis of both the fibrilization and gelation kinetics and their relationship to each other. The general picture of SAFiN formation is the self-assembly of peptides into large aspect ratio fibrils, which at a critical concentration percolate to form a volume spanning network. One has to make a distinction between the kinetics of sheet formation, fibrilization, and gelation. The former two processes can be probed by spectroscopy (IR/VCD and UVCD), while the latter is probed by rheology.

Generally, the kinetics of the self-assembly of peptides and even proteins can be described by a sigmoidal function that reflects the nucleation time and the half time of fibril formation. As shown by Knowles et al. a theory that attempts to account for this behavior must consider nucleation, elongation, and secondary nucleation after fragmentation.<sup>7</sup> Recently, an even more complex approach emphasized the need to consider a conformational change of the peptide during the nucleation phase.<sup>83</sup> General gelation theories such as the classical Flory-Stockmayer theory 78,79 and its later derivatives have not yet been applied to gelation kinetics of the above low molecular weight peptides.

Yokoi et al. measured the fibrilization and gelation kinetics of 3 mM RADA 16 after the sample was fragmented by sonication.<sup>40</sup> The respective kinetic traces are very similar, which suggests that self-assembly is the rate-limiting process. The G' kinetics of Zhao et al. reported for RATEA16 indicate a significant decrease of the effective time constant with increasing peptide concentration, but the data have not been analyzed to further characterize this relationship.<sup>70</sup>

Schneider and co-workers used UVCD and rheology to perform a more thorough kinetic analysis of MAX1 selfassembly and gelation at pH 9.0. The former was found to proceed on a time scale of 10<sup>2</sup> minutes for peptide concentrations of ca. 0.3 mM.<sup>26</sup> Another study showed that the concentration dependence of the gelation time follows a power law with an exponent of -0.9. A follow-up paper by Larsen et al. sheds more light on the parameters that determine MAX1 gelation.<sup>35</sup> They investigated and compared the kinetics

of gelation and self-assembly of MAX1 and MAX1 derivatives where K15 is replaced by Q, T, and E. With 100 mM NaCl gelation of MAX1 starts after 90 min (Figure 15).

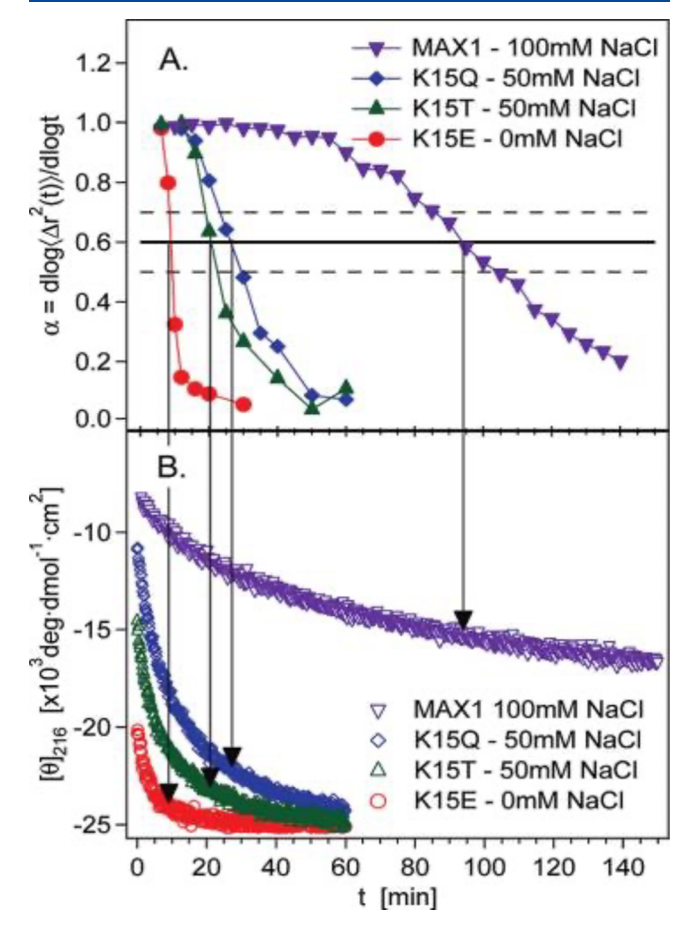


Figure 15. (upper) Gel indicator derived from the time dependence of the slope of the mean-square displacement of the indicated peptides plotted as a function of time. The solid horizontal line indicates the critical value of gelation. (lower) Time dependence of the ellipticity obtained from the UVCD spectrum of the indicated peptides at 218 nm. The vertical errors indicate the time at which the respective gel indicator has reached the critical value. Reprinted with permission from ref 35. Copyright 2009 American Chemical Society.

Simultaneously measured time-resolved UVCD suggests that the self-assembly into  $\beta$ -sheets is nearly completed at that time. This suggests that gel formation occurs on a slower time scale than that of self-assembly. All the above mutants have a drastic effect on both kinetics. The onset of gelation for K15Q, K15T, and K15E were observed at 24, 20, and 9 min. The results reveal how the reduction of positively charged residues and particularly the addition of a negatively charged residue (E) facilitates self-assembly and gelation kinetics. This is an important result in that it shows how gel formation can be designed by choosing the optimal balance of charges.

Several studies of gel kinetics have been performed with Fmoc peptides. Here, we focus on a comprehensive study of the Adler-Abramovich group. Orbach et al. investigated the gelation kinetics of several Fmoc-peptides, among them Fmoc-FF, Fmoc-RGDF, and Fmoc-FG. The data were not further analyzed, but an inspection of the kinetic traces of FmocFF suggests time constants slightly above 100 s for peptide concentrations between 1 and 5 mg/mL (9 and 1.9 mM for

Perspective

FmocFF). Rheological measurements for FmocFF and FmocGF confirmed that gelation proceeds relatively fast on a time scale of several minutes. The utilized concentrations are by an order of magnitude higher than the ones used for MAX1 gelation, but one must take into account that the latter is a much larger peptide with substantially more reaction sites that promote the formation of the folded hairpin conformation (via hydrogen bonding) and fibrils (hydrophobic interactions between side chains).

The kinetics of GAG self-assembly and gelation in waterethanol was studied rather thoroughly. Three different experimental tools were utilized. The kinetics of peptide selfassembly was probed by employing the peculiar amide I profiles in the IR and VCD spectrum of the gel. Generally, VCD is not a suitable technique to probe even slow kinetic processes, since it takes several hours to record a spectrum of peptides with a showable signal-to-noise ratio. However, as already demonstrated by Measey et al., a VCD enhancement caused by chiral fibrils is a game changer, <sup>81</sup> since it allows the recording of a spectrum with sufficient signal-to-noise in less than a minute. Normally, one expects UVCD to be just another indicator of the secondary structure. In the case of GAG self-assembly, several lines of evidence suggest that the peculiar CD spectrum of the gel phase actually probes the formation of fibrils. The kinetics of gelation was probed by rheology.

An analysis of the amide I kinetics suggest that the initial phase of the self-assembly of 200 mM GAG in 55 mol % ethanol/45 mol % water occurs on a time scale of minutes, followed by an order of magnitude slower process. Figure 16 shows the kinetic traces obtained with time-dependent UVCD and rheological measurements for different peptide concentrations and ethanol fractions. The solid lines in the left figures result from a fit to a model of Knowles at al., 69 which takes into account two nucleation processes. The first one is a homogeneous process that accounts for the assembly of monomers into polymers. These polymers can dissociate into an inhomogeneous ensemble of fragments that provide the material for the secondary nucleation. As a consequence, the time dependence of the number of polymers incorporated is described by an exponential function with a time-dependent exponent. In lieu of a comprehensive theory the corresponding gelation kinetics measured by rheology data were fitted with some type of inversed power law (Figure 14, right).<sup>74</sup> A comparison of respective kinetic traces described by DiGuiseppi et al. revealed that, in the initial phase, fibrilization occurs very much on the time scale of the self-assembly process, which indicates that the former determines the overall rate. 69 Both processes become disentangled at lower peptide concentrations or lower ethanol fractions, where gelation takes much more time and thus becomes the rate-limiting process.

The kinetic analysis of GAG self-assembly and gelation reveals the necessity to use different techniques to disentangle between the different processes that eventually lead to gel formation. For gels formed with ultralow molecular weight peptides at very high peptide concentrations there do not exist generalizable relationships between gel strength, kinetic rate constants, and peptide concentration. Instead, the data suggest that a comprehensive theoretical approach must account for the kinetics of the different steps of peptide self-assembly. A validation requires data of the type described in this section.

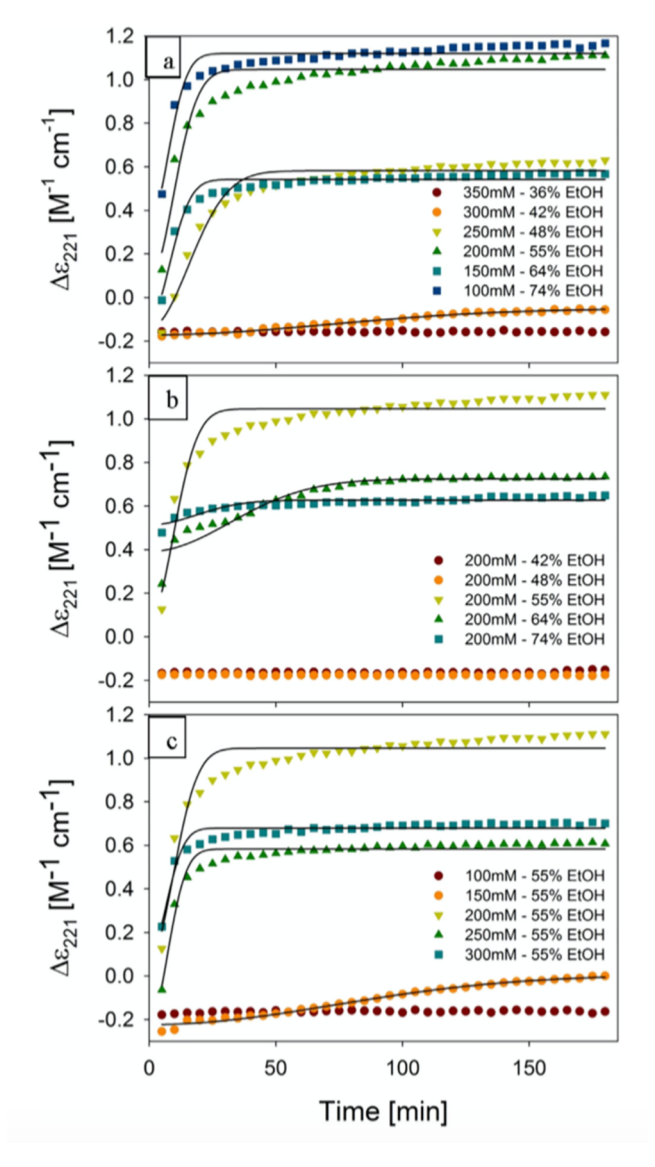


**Figure 16.** Kinetics of GAG fibril formation measured via CD at 221 nm of samples with the indicated GAG concentration and ethanol/water mixture. The solid lines represent the best fit of eq (7) in ref 69. Reprinted from this reference. Copyright 2020 Royal Society of Chemistry.

#### SUMMARY AND OUTLOOK

In many ways, this Perspective has summarized the efforts our laboratories have made in quantifying the gelation of ultrashort unblocked tripeptides using available characterization techniques. As most in the field, we began our tenure with an accidental discovery that GAG and GHG self-assembled into SAFiNs. Note that neither was considered a top candidate for self-assembly in water mixtures. We expect that other GxG peptides containing phenylalanine, tyrosine, and tryptophan as guest residues will promote self-assembly, but this work is still ongoing. A comparison of GAG and GHG networks with other prominent short peptide gelators reveal major differences in terms of the length and thickness of fibrils, the strength and stability of networks, and the kinetics of formation. However, a complete picture is lacking due to insufficient data, particularly regarding the mechanism of self-assembly.

The field of peptide gels is certainly challenging, and the number of fascinating questions remaining should draw the

**PDFelement** 

attention of imaginative and creative researchers. We are far from a framework of peptide gels by chemical design, but additional research and detailed investigations will allow for the testing and validation of models and theories toward this end. This of course requires that the field shift from its current temperament of exploratory research to detailed investigative studies, focusing on the "whys" and "hows". For example, spectroscopic methods offer a detailed evolution of the fibrillization process, especially at the early stages, which allows for a more detailed understanding of the intermolecular forces responsible for self-assembly. Coupling rheology and spectroscopy is a powerful approach in understanding the connection between fibrillization and network structure. However, there is significant room for advancements in techniques and analysis toward this end. Ultimately, we hope that this Perspective stimulates curiosity and sparks other scientists to join the effort.

#### AUTHOR INFORMATION

### **Corresponding Author**

Reinhard Schweitzer-Stenner — Departments of Chemistry, Drexel University, Philadelphia, Pennsylvania 19104, United States; orcid.org/0000-0001-5616-0722; Phone: 1-610-895-2268; Email: rschweitzer-stenner@drexel.edu

#### Author

Nicolas J. Alvarez — Chemical and Biological Engineering, Drexel University, Philadelphia, Pennsylvania 19104, United States

Complete contact information is available at: https://pubs.acs.org/10.1021/acs.jpcb.1c01447

#### Notes

The authors declare no competing financial interest. Biographies



Reinhard Schweitzer-Stenner was born in Herne/Germany. He received his diploma in Physics from the University of Wuppertal (1980), his doctoral degree (Dr rer. nat.) in Physics from the University of Bremen (1983), and his habilitation (venia legendi) from this institution in 1990. After his habilitation he held a faculty position at the University of Bremen until 1999. He worked as a visiting scientist at the Weizmann Institute in Rehovot/Israel (1985/1986) and the University of Michigan in Ann Arbor (1993/1994). In 1999, he became an Associate Professor of Chemistry at the University of Puerto Rico in Rio Piedras. In 2003, he joined the faculty of the Chemistry Department at Drexel University in Philadelphia, where he now holds the rank of a professor. His Biospectroscopy Research Group examines the structure—function

relationship of membrane-bound cytochrome c, determines conformational distributions of peptides, and explores the rules underlying the self-assembly and gelation of low molecular weight peptides.



Nicolas J. Alvarez obtained his BS degree in Chemical Engineering from the University of Florida and his PhD in the same area from Carnegie Mellon University in Pittsburgh, Pennsylvania, in 2011. From 2011 to 2014 he was a Postdoctoral Fellow at the Danish Polymer Center of the Technical University of Denmark in Kongens Lyngby. Subsequently, he joined the Department of Chemical and Biological Engineering of Drexel University as a faculty member, where he now holds the rank of an Associate Professor. His has a variety of research interests in the fields of photonic crystal defect chromatography, extensional rheology of polymer/polymer composites, surfactant/polymer transport to fluid and solid interfaces, aqueous lubrication, and interfacial instabilities.

#### ACKNOWLEDGMENTS

We acknowledge the invaluable contributions of members of the Biospectroscopy Research and the Alvarez Group at Drexel University to the research reported in this Perspective. Spectroscopic work in the Biospectroscopy Research Group was performed by Dr. B. Milorey, S. Farrell, M. Hesser, and Dr. D. DiGuiseppi, who were undergraduate and graduate students of the group. Work in the Alvarez group has been mostly performed by L. Thursch and T. Lewis. Part of the work reported in this Perspective was supported by a National Science Foundation grant to both authors (DMR-1707770).

#### REFERENCES

- (1) Huang, X.; Raghavan, S. R.; Terech, P.; Weiss, R. G. Distinct Kinetic Pathways Generate Organogel Networks with Contrasting Fractality and Thixotropic Properties. *J. Am. Chem. Soc.* **2006**, *128* (47), 15341–15352.
- (2) Weiss, R. G. The Past, Present, and Future of Molecular Gels. What Is the Status of the Field, and Where Is It Going? *J. Am. Chem. Soc.* **2014**, *136* (21), *7519*–*7530*.
- (3) Draper, E. R.; Adams, D. J. Low-Molecular-Weight Gels: The State of the Art. Chem. 2017, 3, 390-410.
- (4) Adler-Abramovich, L.; Gazit, E. The Physical Properties of Supramolecular Peptide Assemblies: From Building Block Association to Technological Applications. *Chem. Soc. Rev.* **2014**, *43*, 6881–6893.
- (5) Seow, W. Y.; Hauser, C. A. E. Short to Ultrashort Peptide Hydrogels for Biomedical Uses. *Mater. Today* **2014**, *17* (8), 381–388.
- (6) Menger, F. M.; Caran, K. L. Anatomy of a Gel. Amino Acid Derivatives That Rigidify Water at Submillimolar Concentrations. *J. Am. Chem. Soc.* **2000**, 122 (47), 11679–11691.
- (7) Hirst, A. R.; Coates, I. A.; Boucheteau, T. R.; Miravet, J. F.; Escuder, B.; Castelletto, V.; Hamley, I. W.; Smith, D. K. Low-

**PDFelement** 

Molecular-Weight Gelators: Elucidating the Principles of Gelation Based on Gelator Solubility and a Cooperative Self-Assembly Model. *J. Am. Chem. Soc.* **2008**, *130* (28), 9113–9121.

- (8) Tantakitti, F.; Boekhoven, J.; Wang, X.; Kazantsev, R. V.; Yu, T.; Li, J.; Zhuang, E.; Zandi, R.; Ortony, J. H.; Newcomb, C. J.; et al. Energy Landscapes and Functions of Supramolecular Systems. *Nat. Mater.* **2016**, *15* (4), 469–476.
- (9) Chiti, F.; Taddei, N.; Baroni, F.; Capanni, C.; Stefani, M.; Ramponi, G.; Dobson, C. M. Kinetic Partitioning of Protein Folding and Aggregation. *Nat. Struct. Biol.* **2002**, *9* (2), 137–143.
- (10) Gsponer, J.; Haberthür, U.; Caflisch, A. The Role of Side-Chain Interactions in the Early Steps of Aggregation: Molecular Dynamics Simulations of an Amyloid-Forming Peptide from the Yeast Prion Sup35. *Proc. Natl. Acad. Sci. U. S. A.* **2003**, *100* (9), 5154–5159.
- (11) Calamai, M.; Canale, C.; Relini, A.; Stefani, M.; Chiti, F.; Dobson, C. M. Reversal of Protein Aggregation Provides Evidence for Multiple Aggregated States. *J. Mol. Biol.* **2005**, *346* (2), 603–616.
- (12) Cheon, M.; Chang, I.; Mohanty, S.; Luheshi, L. M.; Dobson, C. M.; Vendruscolo, M.; Favrin, G. Structural Reorganisation and Potential Toxicity of Oligomeric Species Formed during the Assembly of Amyloid Fibrils. *PLoS Comput. Biol.* **2007**, 3 (9), 1727–1738.
- (13) Auer, S.; Dobson, C. M.; Vendruscolo, M.; Maritan, A. Self-Templated Nucleation in Peptide and Protein Aggregation. *Phys. Rev. Lett.* **2008**, *101* (25), 258101–258104.
- (14) Toriumi, K.; Oma, Y.; Kino, Y.; Futai, E.; Sasagawa, N.; Ishiura, S. Expression of Polyalanine Stretches Induces Mitochondrial Dysfunction. *J. Neurosci. Res.* **2008**, *86* (7), 1529–1537.
- (15) Rovetta, A.; Nasry, I.; Helmi, A. Chariots of the Egyptian Pharaoh Tut Ankh Amun in 1337 B.C.: Kinematics and Dynamics. *Mech. Mach. Theory* **2000**, 35 (7), 1013–1031.
- (16) Cyril P. Bryan, G. E. S. Ancient Egyptian Medicine: The Papyrus Ebers; Ares Publishers, 1930.
- (17) Ando, T.; Yamazaki, Y. Adhesive Crayon Composition Containing Sorbitol-Benzaldehyde Product as Additive. 3,846,363, 1974.
- (18) Palumbo, G.; Preuschen, J. Hydrogel Pressure Sensitive Adhesives for Use as Wound Dressings. EP1051983A1.
- (19) Breton, M. P.; Boils-Boissier, D. C.; Thomas, J. W.; Titterington, D. R.; Goodbrand, H. B.; Banning, J. H.; Wuest, J. D.; Laliberté, D.; Perron, M.-É. Alkylated Urea and Triaminotriazine Compounds and Phase Change Inks Containing Same. 6,860,928, 2005
- (20) Smith, D. K. Applications of Supramolecular Gels. In *Molecular Gels–Structure and Dynamics;* Weiss, R. G., Ed.; Royal Society of Chemistry, 2018; pp 300–371.
- (21) DiGuiseppi, D.; Thursch, L.; Alvarez, N. J.; Schweitzer-Stenner, R. Exploring the Thermal Reversibility and Tunability of a Low Molecular Weight Gelator Using Vibrational and Electronic Spectroscopy and Rheology. *Soft Matter* **2019**, *15* (16), 3418–3431.
- (22) Levine, M. S.; Ghosh, M.; Hesser, M.; Hennessy, N.; Diguiseppi, D. M.; Adler-Abramovich, L.; Schweitzer-Stenner, R. Formation of Peptide-Based Oligomers in Dimethylsulfoxide: Identifying the Precursor of Fibril Formation. *Soft Matter* **2020**, *16* (33), 7860–7868.
- (23) Orbach, R.; Adler-Abramovich, L.; Zigerson, S.; Mironi-Harpaz, I.; Seliktar, D.; Gazit, E. Self-Assembled Fmoc-Peptides as a Platform for the Formation of Nanostructures and Hydrogels. *Biomacromolecules* **2009**, *10* (9), 2646–2651.
- (24) Milorey, B.; Farrell, S.; Toal, S. E.; Schweitzer-Stenner, R. Demixing of Water and Ethanol Causes Conformational Redistribution and Gelation of the Cationic GAG Tripeptide. *Chem. Commun.* **2015**, *51* (92), 16498–16501.
- (25) Farrell, S.; DiGuiseppi, D.; Alvarez, N.; Schweitzer-Stenner, R. The Interplay of Aggregation, Fibrillization and Gelation of an Unexpected Low Molecular Weight Gelator: Glycylalanylglycine in Ethanol/Water. *Soft Matter* **2016**, *12* (28), 6096–6110.
- (26) Schneider, J. P.; Pochan, D. J.; Ozbas, B.; Rajagopal, K.; Pakstis, L.; Kretsinger, J. Responsive Hydrogels from the Intramolecular

- Folding and Self-Assembly of a Designed Peptide. J. Am. Chem. Soc. 2002, 124 (50), 15030-15037.
- (27) Ye, Z.; Zhang, H.; Luo, H.; Wang, S.; Zhou, Q.; Du, X.; Tang, C.; Chen, L.; Liu, J.; Shi, Y. K.; et al. Temperature and PH Effects on Biophysical and Morphological Properties of Self-Assembling Peptide RADA 16–1. *J. Pept. Sci.* **2008**, *14* (2), 152–162.
- (28) Tang, C.; Ulijn, R. V.; Saiani, A. Self-Assembly and Gelation Properties of Glycine/Leucine Fmoc-Dipeptides. *Eur. Phys. J. E: Soft Matter Biol. Phys.* **2013**, 36 (10). DOI: 10.1140/epje/i2013-13111-3
- (29) Aggeli, A.; Bell, M.; Carrick, L. M.; Fishwick, C. W. G.; Harding, R.; Mawer, P. J.; Radford, S. E.; Strong, A. E.; Boden, N. PH as a Trigger of Peptide  $\beta$ -Sheet Self-Assembly and Reversible Switching between Nematic and Isotropic Phases. *J. Am. Chem. Soc.* **2003**, 125 (32), 9619–9628.
- (30) Moyer, T. J.; Finbloom, J. A.; Chen, F.; Toft, D. J.; Cryns, V. L.; Stupp, S. I. PH and Amphiphilic Structure Direct Supramolecular Behavior in Biofunctional Assemblies. *J. Am. Chem. Soc.* **2014**, *136* (42), 14746–14752.
- (31) Hesser, M.; Thursch, L.; Lewis, T.; DiGuiseppi, D.; Alvarez, N. J.; Schweitzer-Stenner, R. The Tripeptide GHG as an Unexpected Hydrogelator Triggered by Imidazole Deprotonation. *Soft Matter* **2020**, *16* (17), 4110–4114.
- (32) Dobson, C. M. Protein Misfolding, Evolution and Disease. *Trends Biochem. Sci.* **1999**, 24 (9), 329–332.
- (33) Frederix, P. W. J. M.; Scott, G. G.; Abul-Haija, Y. M.; Kalafatovic, D.; Pappas, C. G.; Javid, N.; Hunt, N. T.; Ulijn, R. V.; Tuttle, T. Exploring the Sequence Space for (Tri-)Peptide Self-Assembly to Design and Discover New Hydrogels. *Nat. Chem.* **2015**, 7 (1), 30–37.
- (34) Ye, Z.; Zhang, H.; Luo, H.; Wang, S.; Zhou, Q.; Du, X.; Tang, C.; Chen, L.; Liu, J.; Shi, Y. K.; et al. Temperature and PH Effects on Biophysical and Morphological Properties of Self-Assembling Peptide RADA 16–1. *J. Pept. Sci.* **2008**, *14* (2), 152–162.
- (35) Larsen, T. H.; Branco, M. C.; Rajagopal, K.; Schneider, J. P.; Furst, E. M. Sequence-Dependent Gelation Kinetics of  $\beta$ -Hairpin Peptide Hydrogels. *Macromolecules* **2009**, 42 (21), 8443–8450.
- (36) Rajagopal, K.; Schneider, J. P. Self-Assembling Peptides and Proteins for Nanotechnological Applications. *Curr. Opin. Struct. Biol.* **2004**, *14* (4), 480–486.
- (37) Toal, S. E.; Kubatova, N.; Richter, C.; Linhard, V.; Schwalbe, H.; Schweitzer-Stenner, R. Corrigendum: Randomizing the Unfolded State of Peptides (and Proteins) by Nearest Neighbor Interactions between Unlike Residues. *Chem. Eur. J.* **2017**, 23 (71), 18084–18087.
- (38) Chou, P. Y.; Fasman, G. D. Conformational Parameters for Amino Acids in Helical,  $\beta$ -Sheet, and Random Coil Regions Calculated from Proteins. *Biochemistry* **1974**, *13* (2), 211–222.
- (39) Nagy-Smith, K.; Moore, E.; Schneider, J.; Tycko, R. Molecular Structure of Monomorphic Peptide Fibrils within a Kinetically Trapped Hydrogel Network. *Proc. Natl. Acad. Sci. U. S. A.* **2015**, 112 (32), 9816–9821.
- (40) Yokoi, H.; Kinoshita, T.; Zhang, S. Dynamic Reassembly of Peptide RADA16 Nanofiber Scaffold. *Proc. Natl. Acad. Sci. U. S. A.* **2005**, *102* (24), 8414–8419.
- (41) Freeman, R.; Han, M.; Alvarez, Z.; Lewis, J. A.; Wester, J. R.; Stephanopoulos, N.; McClendon, M. T.; Lynsky, C.; Godbe, J. M.; Sangji, H.; et al. Reversible Self-Assembly of Superstructured Networks. *Science (Washington, DC, U. S.)* **2018**, 362 (6416), 808–813.
- (42) Zhang, S.; Lockshin, C.; Cook, R.; Rich, A. Unusually Stable B-sheet Formation in an Ionic Self-complementary Oligopeptide. *Biopolymers* **1994**, 34 (5), 663–672.
- (43) Bakota, E. L.; Aulisa, L.; Galler, K. M.; Hartgerink, J. D. Enzymatic Cross-Linking of a Nanofibrous Peptide Hydrogel. *Biomacromolecules* **2011**, *12* (1), 82–87.
- (44) Moore, A. N.; Hartgerink, J. D. Self-Assembling Multidomain Peptide Nanofibers for Delivery of Bioactive Molecules and Tissue Regeneration. *Acc. Chem. Res.* **2017**, *50* (4), 714–722.

**PDFelement** 

- (45) Measey, T. J.; Schweitzer-Stenner, R. Self-Assembling Alanine-Rich Peptides of Biomedical and Biotechnological Relevance. In *Protein and Peptide Folding, Misfolding, and Non-Folding;* Schweitzer-Stenner, R., Ed.; Wiley & Sons, Inc.: Hoboken, NJ, 2012; pp 307—350
- (46) Tjernberg, L. O.; Näslund, J.; Lindqvist, F.; Johansson, J.; Karlström, A. R.; Thyberg, J.; Terenius, L.; Nordstedt, C. Arrest of β-Amyloid Fibril Formation by a Pentapeptide Ligand. *J. Biol. Chem.* **1996**, 271 (15), 8545–8548.
- (47) Azriel, R.; Gazit, E. Analysis of the Minimal Amyloid-Forming Fragment of the Islet Amyloid Polypeptide. An Experimental Support for the Key Role of the Phenylalanine Residue in Amyloid Formation. *J. Biol. Chem.* **2001**, *276* (36), 34156–34161.
- (48) Mahler, A.; Reches, M.; Rechter, M.; Cohen, S.; Gazit, E. Rigid, Self-Assembled Hydrogel Composed of a Modified Aromatic Dipeptide. *Adv. Mater.* **2006**, *18* (11), 1365–1370.
- (49) Frederix, P. W. J. M.; Ulijn, R. V.; Hunt, N. T.; Tuttle, T. Virtual Screening for Dipeptide Aggregation: Toward Predictive Tools for Peptide Self-Assembly. *J. Phys. Chem. Lett.* **2011**, *2* (19), 2380–2384.
- (50) DiGuiseppi, D.; Schweitzer-Stenner, R. Probing Conformational Propensities of Histidine in Different Protonation States of the Unblocked Glycyl-Histidyl-Glycine Peptide by Vibrational and NMR Spectroscopy. *J. Raman Spectrosc.* **2016**, 47 (9), 1063–1072.
- (51) Ghosh, A.; Tucker, M. J.; Hochstrasser, R. M. Identification of Arginine Residues in Peptides by 2D-IR Echo Spectroscopy. *J. Phys. Chem. A* **2011**, *115* (34), 9731–9738.
- (52) Karjalainen, E. L.; Ravi, H. K.; Barth, A. Simulation of the Amide I Absorption of Stacked β-Sheets. *J. Phys. Chem. B* **2011**, *115* (4), 749–757.
- (53) Kessler, J.; Keiderling, T. A.; Bour, P. Arrangement of Fibril Side Chains Studied by Molecular Dynamics and Simulated Infrared and Vibrational Circular Dichroism Spectra. *J. Phys. Chem. B* **2014**, 118 (24), 6937–6945.
- (54) Kurouski, D.; Lombardi, R. A.; Dukor, R. K.; Lednev, I. K.; Nafie, L. A. Direct Observation and PH Control of Reversed Supramolecular Chirality in Insulin Fibrils by Vibrational Circular Dichroism. *Chem. Commun.* **2010**, *46* (38), 7154–7156.
- (55) Sreerama, N.; Woody, R. W. A Self-Consistent Method for the Analysis of Protein Secondary Structure from Circular Dichroism. *Anal. Biochem.* **1993**, 209 (1), 32–44.
- (56) Woody, R. W. Aromatic Side-chain Contributions to the Far Ultraviolet Circular Dichroism of Peptides and Proteins. *Biopolymers* **1978**, *17* (6), 1451–1467.
- (57) Lee, C.; Cho, M. Local Amide I Mode Frequencies And Coupling Constants in Multiple-Stranded Antiparallel  $\beta$ -Sheet Polypeptides. *J. Phys. Chem. B* **2004**, *108* (52), 20397–20407.
- (58) Schweitzer-Stenner, R. Simulated IR, Isotropic and Anisotropic Raman, and Vibrational Circular Dichroism Amide i Band Profiles of Stacked  $\beta$ -Sheets. *J. Phys. Chem. B* **2012**, *116* (14), 4141–4153.
- (59) Bour, P.; Keiderling, T. A. Structure, Spectra and the Effects of Twisting of  $\beta$ -Sheet Peptides. A Density Functional Theory Study. *J. Mol. Struct.: THEOCHEM* **2004**, *675* (1–3), 95–105.
- (60) Eckes, K. M.; Mu, X.; Ruehle, M. A.; Ren, P.; Suggs, L. J.  $\beta$  Sheets Not Required: Combined Experimental and Computational Studies of Self-Assembly and Gelation of the Ester-Containing Analogue of an Fmoc-Dipeptide Hydrogelator. *Langmuir* **2014**, *30* (18), 5287–5296.
- (61) Toal, S.; Meral, D.; Verbaro, D.; Urbanc, B.; Schweitzer-Stenner, R. PH-Independence of Trialanine and the Effects of Termini Blocking in Short Peptides: A Combined Vibrational, NMR, UVCD, and Molecular Dynamics Study. *J. Phys. Chem. B* **2013**, *117* (14), 3689–3706.
- (62) Hagarman, A.; Measey, T. J.; Mathieu, D.; Schwalbe, H.; Schweitzer-Stenner, R. Intrinsic Propensities of Amino Acid Residues in GxG Peptides Inferred from Amide I' Band Profiles and NMR Scalar Coupling Constants. *J. Am. Chem. Soc.* **2010**, *132* (2), 540–551.

- (63) DiGuiseppi, D.; Milorey, B.; Lewis, G.; Kubatova, N.; Farrell, S.; Schwalbe, H.; Schweitzer-Stenner, R. Probing the Conformation-Dependent Preferential Binding of Ethanol to Cationic Glycylalanylglycine in Water/Ethanol by Vibrational and NMR Spectroscopy. *J. Phys. Chem. B* **2017**, *121* (23), 5744–5758.
- (64) Ilawe, N. V.; Schweitzer-Stenner, R.; Diguiseppi, D.; Wong, B. M. Is a Cross- $\beta$ -Sheet Structure of Low Molecular Weight Peptides Necessary for the Formation of Fibrils and Peptide Hydrogels? *Phys. Chem. Phys.* **2018**, 20, 18158–18168.
- (65) Thursch, L.; Lima, T. A.; Schweitzer-Stenner, R.; Alvarez, N. J. The Impact of Thermal History on the Structure of Glycylalanylglycine Ethanol/Water Gels. J. Pept. Sci. 2021, DOI: 10.1002/psc.3305.
- (66) Fleming, S.; Ulijn, R. V. Design of Nanostructures Based on Aromatic Peptide Amphiphiles. *Chem. Soc. Rev.* **2014**, *43*, 8150–8177.
- (67) Aggeli, A.; Nyrkova, I. A.; Bell, M.; Harding, R.; Carrick, L.; McLeish, T. C. B.; Semenov, A. N.; Boden, N. Hierarchical Self-Assembly of Chiral Rod-like Molecules as a Model for Peptide β-Sheet Tapes, Ribbons, Fibrils, and Fibers. *Proc. Natl. Acad. Sci. U. S. A.* **2001**, 98 (21), 11857–11862.
- (68) Pochan, D. J.; Schneider, J. P.; Kretsinger, J.; Ozbas, B.; Rajagopal, K.; Haines, L. Thermally Reversible Hydrogels via Intramolecular Folding and Consequent Self-Assembly of a de Novo Designed Peptide. J. Am. Chem. Soc. 2003, 125 (39), 11802—11803.
- (69) DiGuiseppi, D. M.; Thursch, L.; Alvarez, N. J.; Schweitzer-Stenner, R. Exploring the Gel Phase of Cationic Glycylalanylglycine in Ethanol/Water. II. Spectroscopic, Kinetic and Thermodynamic Studies. J. Colloid Interface Sci. 2020, 573, 123–134.
- (70) Zhao, Y.; Yokoi, H.; Tanaka, M.; Kinoshita, T.; Tan, T. Self-Assembled PH-Responsive Hydrogels Composed of the RATEA16 Peptide. *Biomacromolecules* **2008**, *9* (6), 1511–1518.
- (71) Tang, C.; Ulijn, R. V.; Saiani, A. Effect of Glycine Substitution on Fmoc-Diphenylalanine Self-Assembly and Gelation Properties. *Langmuir* **2011**, 27 (23), 14438–14449.
- (72) Ozbas, B.; Kretsinger, J.; Rajagopal, K.; Schneider, J. P.; Pochan, D. J. Salt-Triggered Peptide Folding and Consequent Self-Assembly into Hydrogels with Tunable Modulus. *Macromolecules* **2004**, *37* (19), 7331–7337.
- (73) Raeburn, J.; Mendoza-Cuenca, C.; Cattoz, B. N.; Little, M. A.; Terry, A. E.; Zamith Cardoso, A.; Griffiths, P. C.; Adams, D. J. The Effect of Solvent Choice on the Gelation and Final Hydrogel Properties of Fmoc-Diphenylalanine. *Soft Matter* **2015**, *11* (5), 927–935.
- (74) Thursch, L. J.; DiGuiseppi, D.; Lewis, T. R.; Schweitzer-Stenner, R.; Alvarez, N. J. Exploring the Gel Phase of Cationic Glycylalanylglycine in Ethanol/Water. I. Rheology and Microscopy Studies. J. Colloid Interface Sci. 2020, 564, 499–509.
- (75) Li, J. K.; Wang, N.; Wu, X. S. Poly(Vinyl Alcohol) Nanoparticles Prepared by Freezing-Thawing Process for Protein/Peptide Drug Delivery. *J. Controlled Release* **1998**, *56* (1–3), 117–126
- (76) Stammen, J. A.; Williams, S.; Ku, D. N.; Guldberg, R. E. Mechanical Properties of a Novel PVA Hydrogel in Shear and Unconfined Compression. *Biomaterials* **2001**, 22 (8), 799–806.
- (77) Knowles, T. P. J.; Waudby, C. A.; Devlin, G. L.; Cohen, S. I. A.; Aguzzi, A.; Vendruscolo, M.; Terentjev, E. M.; Welland, M. E.; Dobson, C. M. An Analytical Solution to the Kinetics of Breakable Filament Assembly. *Science (Washington, DC, U. S.)* **2009**, 326 (5959), 1533–1537.
- (78) Flory, P. J. Molecular Size Distribution in Three Dimensional Polymers. I. Gelation. J. Am. Chem. Soc. 1941, 63 (11), 3083–3090.
- (79) Stockmayer, W. H. Theory of Molecular Size Distribution and Gel Formation in Branched-Chain Polymers. *J. Chem. Phys.* **1943**, *11* (2), 45–55.
- (80) Veerman, C.; Rajagopal, K.; Palla, C. S.; Pochan, D. J.; Schneider, J. P.; Furst, E. M. Gelation Kinetics of  $\beta$ -Hairpin Peptide Hydrogel Networks. *Macromolecules* **2006**, 39 (19), 6608–6614.
- (81) Measey, T. J.; Schweitzer-Stenner, R. Vibrational Circular Dichroism as a Probe of Fibrillogenesis: The Origin of the Anomalous

# The Journal of Physical Chemistry B

pubs.acs.org/JPCB

Perspective

Intensity Enhancement of Amyloid-like Fibrils. J. Am. Chem. Soc. 2011, 133 (4), 1066–1076.

- (82) Gazit, E. Self-assembled peptide nanostructures: the design of molecular building blocks and their technological utilization. *Chem. Soc. Rev.* **2007**, *36*, 1263–1269.
- (83) Schreck, J. S.; Yuan, J.-M. A Kinetic Study of Amyloid Formation: Fibril Growth and Length Distributions. *J. Phys. Chem. B* **2013**, *117*, 6574–6583.
- (84) Bera, S.; Mondal, S.; Xue, B.; Shimon, L. J. W.; Cao, Y.; Gazit, E. Rigid helical-like assemblies from a self-aggregating tripeptide. *Nat. Mater.* **2019**, *18*, 503–509.